Forces Driving the Binding of Homeodomains to DNA†

Anatoly I. Dragan, Zhenlan Li, Elena N. Makeyeva, Ekaterina I. Milgotina, Yingyun Liu, Colyn Crane-Robinson,‡ and Peter L. Privalov*

Department of Biology, Johns Hopkins University, Baltimore, Maryland 21218

Received August 25, 2005; Revised Manuscript Received October 17, 2005

ABSTRACT: Homeodomains are helix−turn−helix type DNA-binding domains that exhibit sequence-specific DNA binding by insertion of their "recognition" α helices into the major groove and a short N-terminal arm into the adjacent minor groove without inducing substantial distortion of the DNA. The stability and DNA binding of four representatives of this family, MATα2, engrailed, Antennapedia, and NK-2, and truncated forms of the last two lacking their N-terminal arms have been studied by a combination of optical and microcalorimetric methods at different temperatures and salt concentrations. It was found that the stability of the free homeodomains in solution is rather low and, surprisingly, is reduced by the presence of the N-terminal arm for the Antennapedia and NK-2 domains. Their stabilities depend significantly upon the presence of salt: strongly for NaCl but less so for NaF, demonstrating specific interactions with chloride ions. The enthalpies of association of the homeodomains with their cognate DNAs are negative, at 20 °C varying only between −12 and −26 kJ/mol for the intact homeodomains, and the entropies of association are positive; i.e., DNA binding is both enthalpy- and entropy-driven. Analysis of the salt dependence of the association constants showed that the electrostatic component of the Gibbs energy of association resulting from the entropy of mixing of released ions dominates the binding, being about twice the magnitude of the nonelectrostatic component that results from dehydration of the protein/DNA interface, van der Waals interactions, and hydrogen bonding. A comparison of the effects of NaCl/KCl with NaF showed that homeodomain binding results in a release not only of cations from the DNA phosphates but also of chloride ions specifically associated with the proteins. The binding of the basic N-terminal arms in the minor groove is entirely enthalpic with a negative heat capacity effect, i.e., is due to sequence-specific formation of hydrogen bonds and hydrophobic interactions rather than electrostatic contacts with the DNA phosphates.

The eukaryotic homeotic transcription factors and bacterial repressors contain DNA-binding domains (DBDs) of the helix−turn−helix type that exhibit sequence-specific DNA binding by insertion of their "recognition" α helices into the major groove of DNA and a short extended N- or C-terminal arm into the adjacent minor groove (Figure 1) (*1*−*8*). Binding does not result in noticeable deformation of the DNA, although some changes in the structure of the homeodomains have been reported, particularly in the DNA recognition helix (*7*−*11*). Several calorimetric studies have been carried out to determine the energetics of association of the homeodomains and bacterial repressor DBDs with DNA duplexes containing their recognition sequences (*9*, *12*−*17*). These have shown a broad range of enthalpies and entropies of binding that do not obviously correlate with their association constants, which in fact do not vary greatly. In all cases, a negative enthalpy (ΔH) was reported but this varied from −80 and −95 kJ/mol for MATα2 and λcI to −28 kJ/mol for NK2 and ∼ −10 kJ/mol estimated for Antennapedia homeodomain from *Drosophila* (Antp).[1] A negative heat capacity change (ΔC_p) was observed in almost all cases (from −3.9 kJ mol^{-1} K^{-1} for the trp repressor to about −1.0 kJ mol^{-1} K^{-1} for Antp), although for the NK2 homeodomain a positive value of ΔC_p (∼ +1.0 kJ mol^{-1} K^{-1}) was reported (*12*). This range of binding parameters is unexpected, bearing in mind the similarity in the modes of binding of these DBDs and the absence of major DNA distortion.

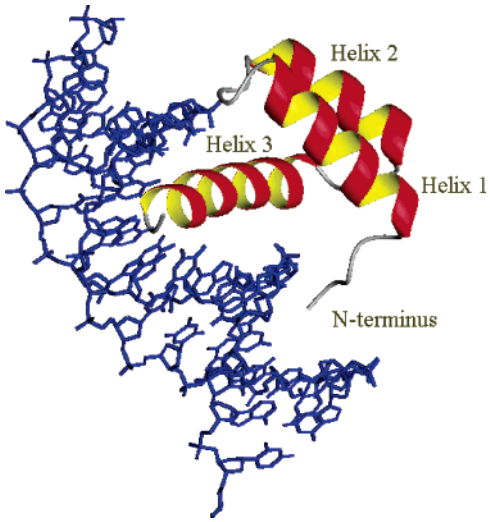

FIGURE 1: Crystal structure of the Antennapedia homeodomain complex with DNA showing the recognition helix in the major groove and the N-terminal arm inserted into the minor groove. The coordinates were taken from PDB 9ANT (*48*).

† This work was supported by NIH Grant GM48036-12.

* To whom correspondence should be addressed. E-mail: privalov@jhu.edu. Telephone: 410-516-6532.

‡ Permanent address: Biophysics Laboratories, University of Portsmouth, Portsmouth PO1 2DT, U.K.

10.1021/bi051705m CCC: $33.50
Published on Web 12/07/2005

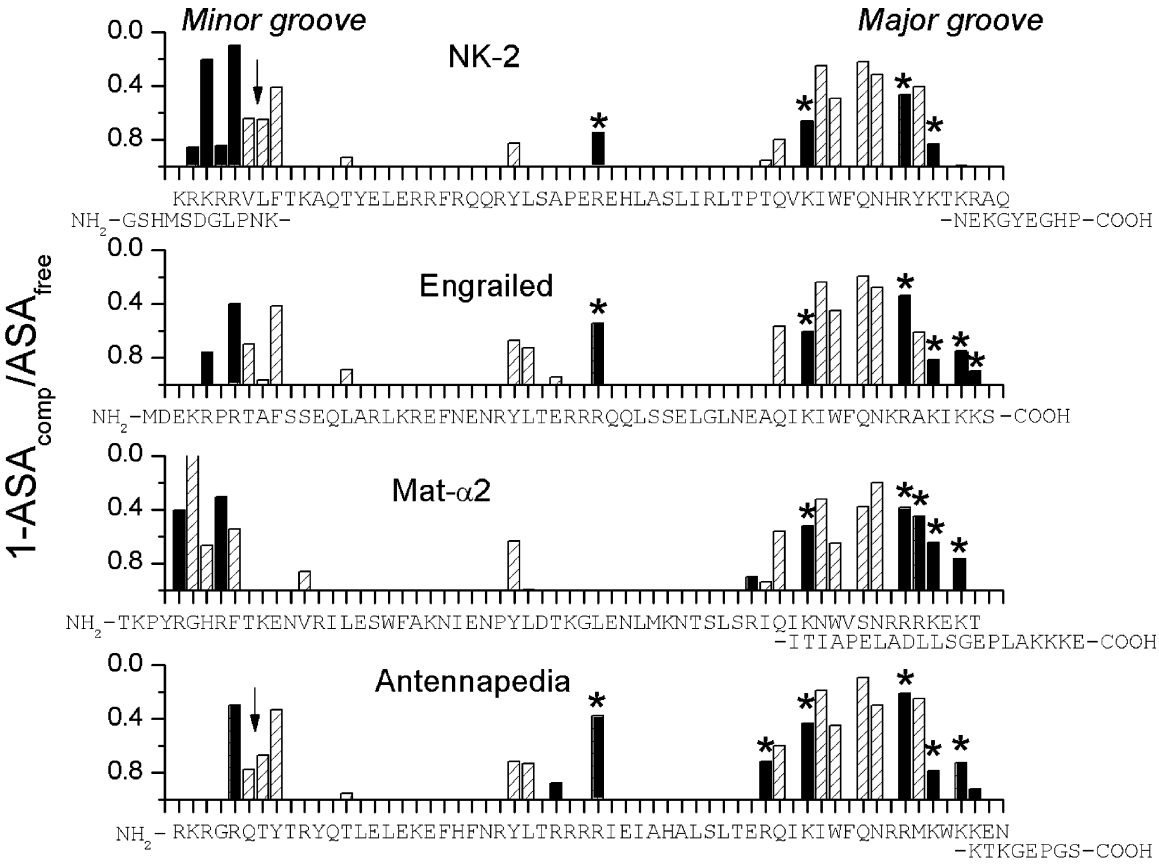

FIGURE 2: Sequence of the studied homeodomains and their contact diagrams in the complexes with DNA expressed as the relative reduction of the ASA of the individual residues in the presence of DNA, with respect to the free protein, determined from the known structures of their complexes (*1*−*3*, *8*, *48*) using the NACCESS 2.1.1 program (http//wolf.tms.umist.ac.uk/naccess/) and the following PDB files: Antp, 9ANT; NK2, 1NK3; engrailed, 3HDD; Matα2, 1APL. The dashed bars show all protein/DNA contacts; the black bars show the contacts of Arg and Lys residues with DNA; and the asterisks indicate contacts of Arg and Lys with the DNA phosphates. Arrows in the case of NK-2 and Antp show the N-terminal truncation sites in the desNK-2 and desAntp homeodomains.

This study was conducted, using just homeodomains, to understand the basis of this wide variation in binding energetics and thereby define the forces driving the binding of helix−turn−helix DBDs to DNA. Three possible causes of the variation were apparent: (1) there might be significant variation in the amount of refolding and induced fit in the DBDs on binding DNA; (2) the N-terminal arms, disordered in free solution but bound into the minor groove in the complexes, might make a significant and variable contribution to the binding energetics; and (3) major differences might exist in the relative contributions from the electrostatic and nonelectrostatic components of the binding energy. Additionally, changes in histidine ionization on forming the protein/DNA complex could be a contributor to the binding enthalpy for certain homeodomains if the pH used was in the range of about 6−7.

Four different examples of homeodomains were studied: *Drosophila* engrailed, *Saccharomyces cerevisiae* MATα2, *Drosophila* Antennapedia, and *Drosophila* NK2, the last two of which were also investigated in truncated forms lacking their N-terminal arms. Three specific strategies were adopted: the first to measure the degree of protein refolding by optical methods and then make an appropriate correction to the measured binding enthalpies; the second to compare intact and truncated versions of two of the homeodomains; and the third to use our established salt-titration methodology to separate the total Gibbs energy of binding into its electrostatic and nonelectrostatic components.

MATERIALS AND METHODS

Proteins. The homeodomain fragments containing the DNA-binding domain were the 68-residue Antp and a truncated form lacking the first six N-terminal residues (desAntp), the 80-residue *Drosophila* NK-2 homeodomain (NK-2) and a truncated form lacking the first 17 N-terminal residues (desNK-2), the 61-residue *Drosophila* engrailed homeodomain (Engr), and the 82-residue yeast MATα2 homeodomain (MATα2). The sequences of these homeodomains are given in Figure 2, which also shows the extent of the contacts of each residue with DNA and particularly of the basic residues (Lys and Arg), determined from the known structures of the free and bound homeodomains, expressed as the reduction of their water-accessible surface areas (ASA).

All of the homeodomains were expressed and isolated as described elsewhere (*9*, *18*). The purity of the expressed proteins was checked by SDS gel electrophoresis, and the

[1] Abbreviations: Antp, Antennapedia homeodomain from *Drosophila*; desAntp, truncated form of Antennapedia homeodomain lacking the first 6 N-terminal residues; NK-2, *Drosophila* NK-2 homeodomain; desNK-2, truncated form lacking the first 17 N-terminal residues; Engr, *Drosophila* engrailed homeodomain; MATα2, yeast MATα2 homeodomain; FAM, 5,6-carboxyfluorescein; ASA, water-accessible surface area; C_p, partial molar heat capacity; ΔH^a, ΔS^a, and ΔG^a, enthalpy, entropy, and Gibbs energy of association.

molecular masses were verified by mass spectrometry. The purity of all of the preparations used was better than 98%. Protein concentrations were determined by UV spectroscopy using the following extinction coefficients: Antennapedia DBDs, $\epsilon_{280} = 15\,220\ M^{-1}\ cm^{-1}$; engrailed DBD, $\epsilon_{280} = 6970\ M^{-1}\ cm^{-1}$; NK-2 DBDs, $\epsilon_{280} = 10\,810\ M^{-1}\ cm^{-1}$; MATα2 DBD, $\epsilon_{280} = 19\,750\ M^{-1}\ cm^{-1}$. Most of the results reported were obtained in 20 mM Na/acetate at pH 5.0 and 100 mM NaCl, conditions that avoid aggregation, which is significant in neutral solution.

DNA Duplexes. The single strands were synthesized by IDT, Inc. Concentrations were determined by measuring the extinction coefficients at 260 nm after complete digestion by phosphodiesterase I in 100 mM Tris-HCl at pH 8.0. To prepare duplexes, equimolar amounts of the complementary strands were mixed, heated at 90 °C for 10 min, and slowly cooled to room temperature. For the calorimetric experiments, 18-bp duplexes were used, and for the fluorescence anisotropy titrations, 14-bp duplexes were used, in which one of the strands is 5′-labeled with FAM. Because the recognition sites of the considered homeodomains are different, the following duplexes were used in this study:

(a) For engrailed:

5′-GCG GGT AAT TAC ATG CGC-3′
3′-CGC CCA TTA ATG TAC GCG-5′

FAM-5′-G GGT AAT TAC ATG C-3′
3′-C CCA TTA ATG TAC G-5′

(b) For Antennapedia:

5′-GCG AAA GCC ATT AGA GCG-3′
3′-CGC TTT CGG TAA TCT CGC-5′

FAM-5′-G AAA GCC ATT AGA G-3′
3′-C TTT CGG TAA TCT C-5′

(c) For MATα2:

5′-GCG GAC ATG TAA TTC GCG-3′
3′-CGC CTG TAC ATT AAG CGC-5′

FAM-5′-G GAC ATG TAA TTC G-3′
3′-C CTG TAC ATT AAG C-5′

(d) For NK-2:

5′-GCG GTG TCA AGT GGC TGG-3′
3′-GCG CAC AGT TCA CCG ACC-5′

FAM-5′-GTG TCA AGT GGC TG-3′
3′-CAC AGT TCA CCG AC-5′

Differential Scanning Calorimetry (DSC). The DSC studies were carried out using a platinum capillary Nano-DSC instrument (CSC, Utah) with a cell volume of 0.328 mL. Details of the performance of this instrument and the experimental procedures are given elsewhere (*19*, *20*). Solutions for the calorimetric experiments were extensively dialyzed against the solvent for 12 h at 5 °C with three replacements of dialyzate, using protein concentrations of ~0.2 mM. The dialyzate was used as the reference. The heat capacity function expected for the fully folded proteins was calculated from the partial specific heat capacity of BPTI, a compact and highly stable protein (*21*, *22*). The heat capacity function expected for the fully unfolded protein was calculated by summing the known tabulated heat capacities of the individual amino acid residues (*23*, *24*). The measured heat capacity functions were analyzed by the CpCalc program, which is provided by CSC.

Isothermal Titration Calorimetry (ITC). ITC was performed on a Nano-ITC Series III from Calorimetry Sciences Corporation (CSC, Utah) with a cell volume of 1.0 mL. DNA solutions were placed in the cell, and concentrated protein solutions were placed in the syringe. The protein solution was titrated in 5 μL increments at 200 s intervals into the DNA solution, using DNA concentrations of ~16 μM in the cell and protein concentrations at ~200 μM in the syringe.

Solutions of DNA and protein were prepared with the same batch of buffer to minimize artifacts because of minor differences in buffer composition. In separate experiments, the heats of dilution of the protein into the solvent were measured and corrections were made. The results of titration experiments were analyzed using the Bindwork program supplied with the instrument.

Spectropolarimetry. CD measurements were carried out using a Jasco-710 spectropolarimeter equipped with a Peltier temperature controller PTC-3481. Measurements of the ellipticity and melting of the samples were made in a 1 mm Suprasil quartz cell in 20 mM Na/acetate at pH 5.0 and 100 mM NaCl using concentrations of the proteins, DNA, and complexes on the order of 10 μM.

Fluorescence Anisotropy Titration. Fluorescence anisotropy, corrected for the *G* factor, was measured on a SPEX FluoroMax-3 spectrofluorimeter under control of DataMax software (version 2.10). Excitation and registration of emission were at 490 and 520 nm, respectively. The instrument has a thermostated cell holder with a magnetic stirrer and software-controlled water bath. All measurements were conducted in 20 mM Na/acetate at pH 5.0 containing different NaCl concentrations at 20 °C. The concentration of DNA duplexes in the titration experiments varied from 20 to 100 nM. Association constants were evaluated by direct fitting of measured binding isotherms as previously described (*25*). The fitting procedure assumed a 1:1 equilibrium between free homeodomains and DNA.

RESULTS

Stability of Free Homeodomains and Their Complexes. Stability studies of all of the considered homeodomains were carried out in slightly acidic solutions (pH 5.0) rather than close to neutral pH: this does not noticeably decrease the stability of the proteins (less than 0.5 K) but prevents their aggregation upon unfolding, which is important for equilibrium analysis of this process. Figure 3a shows the DSC-measured partial specific heat capacity functions of NK-2 and Antp and their truncated forms in solutions of 20 mM sodium acetate at pH 5.0 and 100 mM NaCl. These profiles, which were obtained upon heating with a rate of 1 K/min are perfectly reproducible in subsequent cooling experiments if the solution is not heated above 70 °C. One can therefore

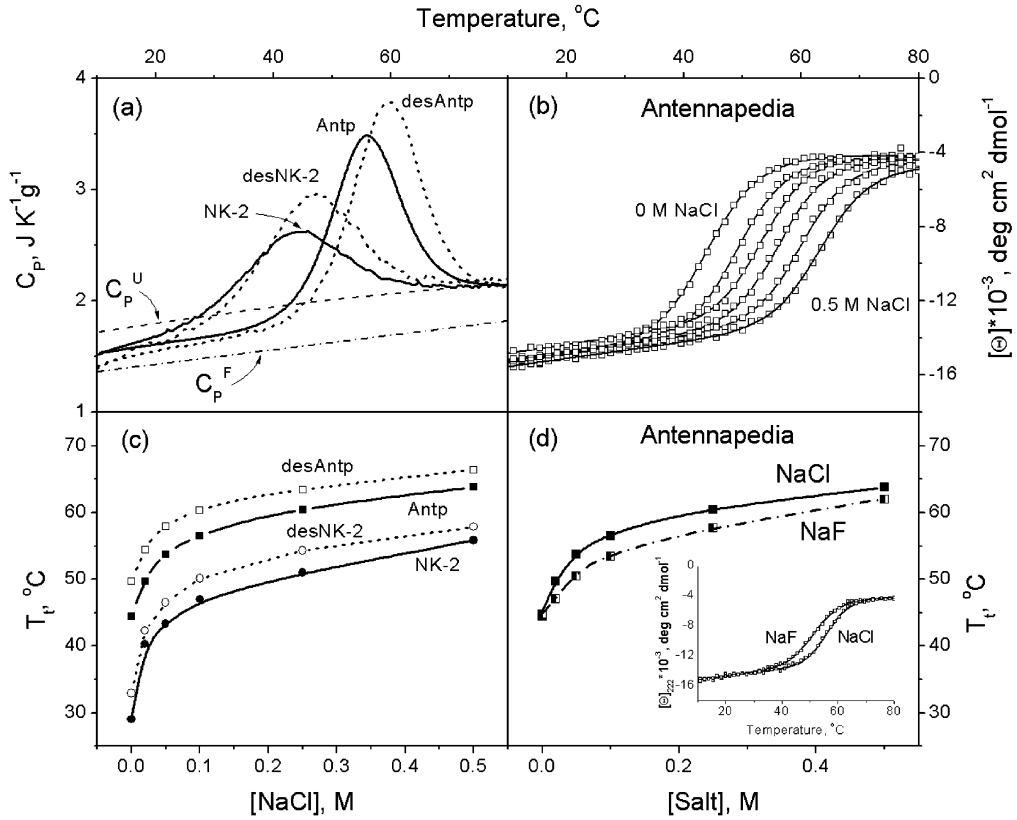

FIGURE 3: (a) Partial specific heat capacity functions of the NK-2, Antp (—), and their truncated forms desNK-2 and desAntp (- - -) in 20 mM sodium acetate buffer at pH 5.0 and 100 mM NaCl. The heat capacity functions expected for the fully folded proteins, C_p^F, and fully unfolded proteins, C_p^U are shown. (b) CD melting profiles, measured at 222 nm, of Antp in the presence of increasing in 0.1 M steps of the concentration of NaCl. (c) Dependence of the transition temperatures, T_t, of Antp and NK-2 (—) and their truncated forms (- - -) on the concentration of NaCl. (d) Dependence of the transition temperature of Antp on the concentration of NaCl and NaF. The inset compares the thermal transitions of Antp in 0.1 M NaCl and 0.1 M NaF, monitored by CD. All measurements were done in 20 mM sodium acetate buffer at pH 5.0.

conclude that the temperature-induced unfolding of these proteins, which proceeds with significant heat absorption, is highly reversible. This figure also shows the heat capacity functions expected for the fully folded proteins, C_p^F, and for the fully unfolded proteins, C_p^U. The heat capacity of the fully unfolded homeodomains was calculated by summing up the heat capacities of the constituent amino acid residues (see the Materials and Methods). These C_p^U functions do not differ much for all of the homeodomains and on the scale used cannot be distinguished. The heat capacity expected for the fully folded proteins, C_p^F, was derived previously (e.g., see ref *26*) from the specific heat capacity of BPTI, a highly stable protein with a compact rigid structure (*21*). It is seen that the heat capacities of the native homeodomains increase gradually, with slopes that do not differ much from that expected for a protein with a compact rigid structure, such as BPTI, but are somewhat higher in absolute magnitude, as expected because the structure of homeodomains is not 100% compact but contains unfolded segments. In the case of the Antennapedia homeodomain, the NMR structure shows that these are the N-terminal residues 1−9 and C-terminal residues 60−67 (*6*). The C_p/T functions at low temperatures show that the extent of these unfolded parts does not significantly increase with heating below the point of temperature-induced cooperative unfolding of the compact domains, which proceeds with an extensive heat absorption and significant heat capacity rise to the level expected for fully unfolded polypeptides. Analysis of the excess heat absorption shows that this process is reversible and is well-approximated by a two-state transition; i.e., in pH 5.0 solutions, we did not find the deviations between the van't Hoff and calorimetric enthalpies that were reported for the NK-2 homeodomain in pH 7.4 solutions (*12*).

Table 1: Thermodynamic Characteristics of the Free Homeodomains in 20 mM Na/Acetate at pH 5.0 and 100 mM NaCl

protein	T_t (°C)	ΔH_t (kJ/mol)	ΔC_p [kJ/(K mol)]	ΔG (20 °C) (kJ/mol)
NK-2	42.1	154	1.6	9.4
desNK-2	45.5	166	1.5	11.7
engrailed	48.7	154	1.5	11.7
MATα2	52.2	197	1.9	16.4
Antp	55.5	226	1.2	22.0
desAntp	59.0	232	1.2	24.2
σ	±0.1	±7	±0.2	±1.3

It is notable that the several homeodomains differ significantly in stability: NK-2 is the most unstable and starts to unfold from 20 °C, and its transition temperature is at 42.1 °C. The most stable is desAntp, the transition temperature of which is 59 °C. The stabilities of the other homeodomains lie in between, and the Gibbs energies of their stabilization vary from 9 to 24 kJ/mol at 20 °C (Table 1). It is striking that the stabilities of the truncated forms of Antp and NK-2, lacking their N-terminal arms, are higher than the full-length parent homeodomains by about 2 kJ/mol.

The stability of the homeodomains depends upon the concentration of NaCl (Figure 3b). It is interesting that the

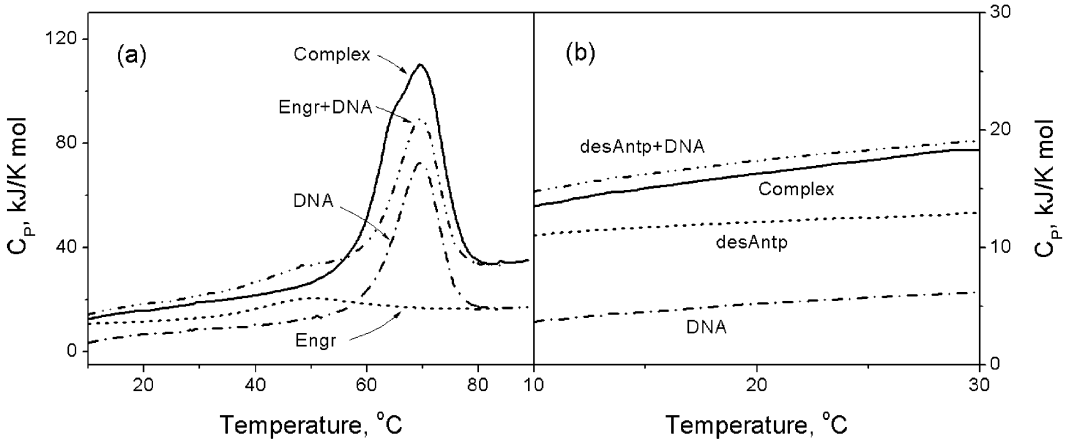

FIGURE 4: (a) Heat capacity functions of the free engrailed DBD, free DNA, their 1:1 complex, and the summed heat capacities of the free protein and free DNA. (b) Partial heat capacities of Antp, its target DNA duplex, and their complex in the temperature range from 10 to 30 °C, given on an enlarged scale and measured using especially concentrated solutions. All DSC experiments were carried out in 100 mM NaCl and 20 mM sodium acetate at pH 5.0.

increase of the salt concentration does not affect the difference in the stabilities of the full and truncated forms of the two homeodomains, Antp and NK-2 (Figure 3c). It appears thus that the interactions between the highly charged N-terminal arms and the globular parts are not of an electrostatic nature. Another notable feature of the homeodomains is that the influence of NaCl and NaF on their stability is different: the stabilizing effect of the chloride salt is stronger (Figure 3d); i.e., the chloride anion binds more strongly to the folded homeodomains than does the fluoride anion (see also below).

Stability of the Homeodomain Complexes. The association of homeodomains with their cognate DNA duplexes significantly stabilizes their structure, and Figure 4 illustrates this with the engrailed complex. The heat capacity profile of the complex shows no sign of free protein melting at around 49 °C but instead a heat absorption peak of a complex shape with a maximum at 70 °C, coinciding with the melting of the free DNA, and a shoulder at ~65 °C, corresponding to the dissociation and melting of the protein. It is notable that the heat capacity function of the complex is almost parallel to the summed heat capacity of the protein and DNA below 30 °C, the temperature at which the protein starts to unfold; i.e., at temperatures below that of cooperative unfolding, heating does not induce significant structural changes in the complex. This is illustrated on an enlarged scale in Figure 4b for Antp, using more concentrated solutions to improve the accuracy. Because Antp is the most stable homeodomain, it allows the heat capacity function of the native state at low temperatures to be determined over a broader temperature range. This demonstrates that, like engrailed, there are no significant changes in the structure over this range, neither in the protein nor the DNA, and because the summed and observed heat capacity functions are parallel, no corrections for refolding of the components need to be made to ITC-measured enthalpies of binding.

Conformational Changes upon Binding. Reports in the literature indicate that, for certain homeodomains, binding to DNA results in an increase in the length of their recognition helices (*7*). Because this might contribute significantly to the energetics of complex formation, we used CD to check that this indeed occurs with the homeodomains studied here. Figure 5 depicts the CD spectra of the free

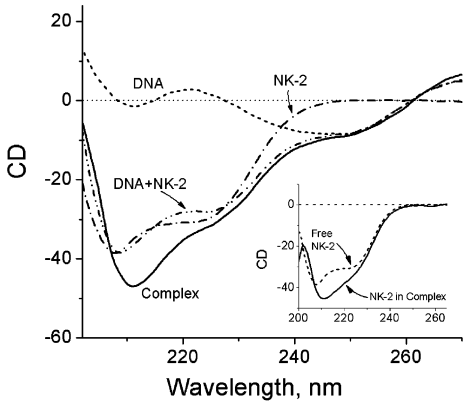

FIGURE 5: CD spectra of the free NK-2 homeodomain, free DNA, and their complex. (Inset) Spectrum of free NK-2 (—) and NK2 in its complex with DNA (- - -), i.e., with the contribution of DNA subtracted.

NK-2 homeodomain, free DNA, and their 1:1 complex, and the inset compares the spectrum of the free protein with the protein in its DNA complex, i.e., corrected for the contribution of the DNA assuming that it does not change. It can be seen that in the presence of 100 mM NaCl binding to DNA changes the helicity of NK-2 by about 20%, and because the free protein contains a total of 35 helical residues, this implies an increase of 7 helical residues. A similar situation was found for the MATα2 homeodomain: its helicity also changes by about 20% on binding to DNA (*9*), which likewise corresponds to an increase of 7 helical residues. For the other homeodomains studied, Antp and Engr, no structural changes have been reported upon binding DNA nor was any change in conformation observed by CD (data not shown).

Enthalpies of Binding. Figure 6a shows the enthalpies of binding the homeodomains to their cognate DNAs, measured by ITC at different temperatures in 100 mM NaCl and 20 mM sodium acetate at pH 5.0. The binding enthalpies are largely negative over the considered temperature range, and their magnitude increases with the temperature rise. The values of these enthalpies vary considerably for the different complexes, lying between −7 and −50 kJ/mol at 20 °C, but their initial temperature dependencies are similar. For the NK-2 homeodomain, the binding enthalpy and its temperature dependence differ from that reported at pH 7.4 (*12*).

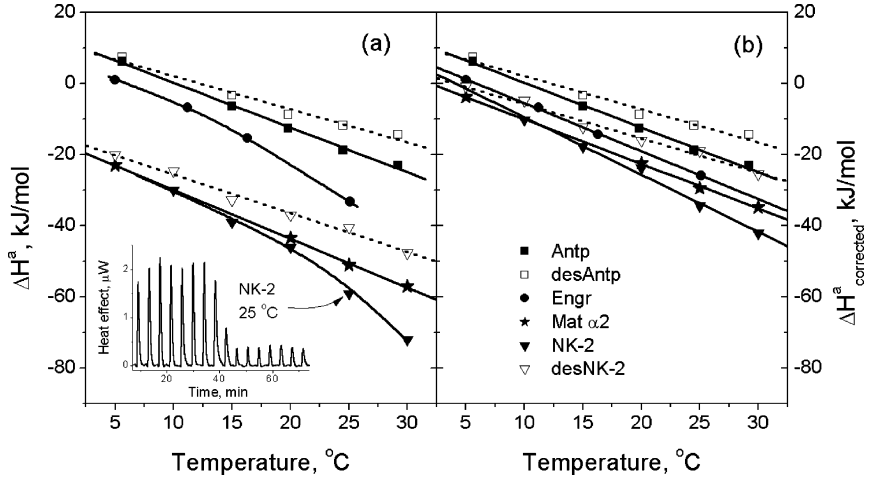

FIGURE 6: (a) Enthalpies of association of the homeodomains and their truncated forms (- - -) with their cognate DNAs measured by ITC at different temperatures. (Inset) Traces of the calorimetric titration of 16 μM DNA by NK-2 at 25 °C. (b) Enthalpies of association of the homeodomains after correcting NK-2 and MATα2 for the heats of refolding of seven residues in their recognition helices and in the case of NK-2 for some further protein refolding that occurs upon binding. All of the data shown were obtained in 100 mM NaCl and 20 mM sodium acetate at pH 5.0.

In this context, it is worth noting that the binding enthalpy of Engr does not change noticeably upon increasing the pH from 5.0 to 7.0, while those of Antp, NK-2, and MATα2 increase in magnitude by 15−20 kJ/mol (data not shown). This change of binding enthalpy is caused by histidines located at the binding sites of these three homeodomains: binding changes their pK_a, resulting in protonation. Studies of homeodomain binding at pH 5.0 avoid this complication.

It is noticeable that the binding enthalpy functions of the homeodomains (Figure 6a) are grouped in two distinct bunches: binding of MATα2 and NK-2, the latter, both full length and truncated, is specified by more negative enthalpies than those of Engr, Antp, and desAntp. As discussed above, the DNA binding of MATα2 and NK-2 is accompanied by an increase in the length of their recognition helices by about 7 residues. Taking the enthalpy of folding an α helix is about 3 kJ/(mol of residue) (*27*), refolding of these proteins upon binding to DNA results in a release of ∼21 kJ/mol; therefore, a positive correction of this magnitude has been applied to these two homeodomains. A small additional correction for refolding must also be introduced for NK-2, which starts to unfold at temperatures above 20 °C but refolds upon binding to DNA (see Figure 3). Introducing all of these corrections, we find that the enthalpies of DNA association of all of the completely folded homeodomains and their temperature dependencies (i.e., the heat capacity effects of binding) no longer cover a broad range (Figure 6b and Table 2).

If the binding enthalpies for the Antp and NK-2 DBDs are compared with those of their truncated forms, it is seen that they differ significantly (Figure 6b). For Antp, removal of the 6 N-terminal residues (RKRGRQ) reduces the binding enthalpy at 20 °C by 5 kJ/mol from −12 to −7 kJ/mol. In the case of NK-2, removal of its longer N-terminal arm, of which only the 7 residues KKRKRRV make contact with DNA, reduces the binding enthalpy at 20 °C by 8 kJ/mol from −24 to −16 kJ/mol. Thus, the N-terminal arms, which enter into the minor groove, contribute a significant negative enthalpy to the binding (Table 2). It is notable that the N-terminal arms also change the slopes of the enthalpy functions: the temperature dependence of the enthalpy is less for desAntp and desNK-2 than for the full-length homeodomains. Thus, the heat capacity effect (ΔC_p) of binding the arms to the minor groove is negative.

Table 2: Binding Characteristics of Homeodomains to Their Cognate DNAs at 20 °C in 100 mM NaCl and 20 mM Na/Acetate Buffer at pH 5.0[a]

protein	ΔH^a	$\Delta C_p{}^a$	$\log(K^a)$	$(\partial \log(K^a))/(\partial \log [\mathrm{NaCl}])$	$\log(K^a)_o$
Antp	−12.0	−1.26	9.7	−6.9	2.8
desAntp	−7.0	−0.93	8.5	−7.0	1.5
NK-2	−24.0	−1.60	9.1	−5.5	3.6
desNK-2	−16.0	−0.97	7.2	−5.6	2.9
MATα2	−26.0	−1.25	8.9	−5.8	3.1
engrailed	−19.0	−1.35	8.1	−6.6	1.5
σ	±1.0	±0.10	±0.2	±0.3	±0.2

[a] ΔG and ΔH are in kJ/mol. ΔC_p is in kJ/(K mol). ΔH values were obtained from ITC measurements. ΔC_p values are obtained as the slopes of the $\Delta H/T$ functions after correction for protein refolding (Figure 6b). Values of K^a and $(\partial \log(K^a))/(\partial \log [\mathrm{NaCl}])$ were obtained from binding curves determined by fluorescence anisotropy titrations at different NaCl concentrations. $(K^a)_o$ is the value of K^a extrapolated to a 1 M NaCl concentration, i.e., $\log[\mathrm{NaCl}] = 0$ (e.g., parts b and d of Figure 7).

Association Constants and Their Dependence on the Ionic Strength. The DNA affinities of all of the homeodomains are quite high, with K_d values being in the nanomolar range; therefore, they cannot be determined from ITC experiments, which require the use of much higher concentrations of the reactants. For determination of the binding isotherms, we therefore used the method of fluorescence anisotropy titration. When the terminal base of the DNA duplexes is labeled with a fluorophore (see the Materials and Methods) and a sensitive spectrofluorimeter is used, binding of the protein to DNA can be monitored using the change in polarization of fluorescence at very low concentrations. As an example, Figure 7a shows the salt titrations of the Antp and desAntp complexes, from which it is seen that the desAntp complex starts to dissociate at a significantly lower concentration of salt than full Antp. The association constants calculated from these experiments are presented in Figure 7b on a logarithmic scale, showing that the dependences of $\log(K^a)$ on log [NaCl] are linear. A similar linearity was found for the other

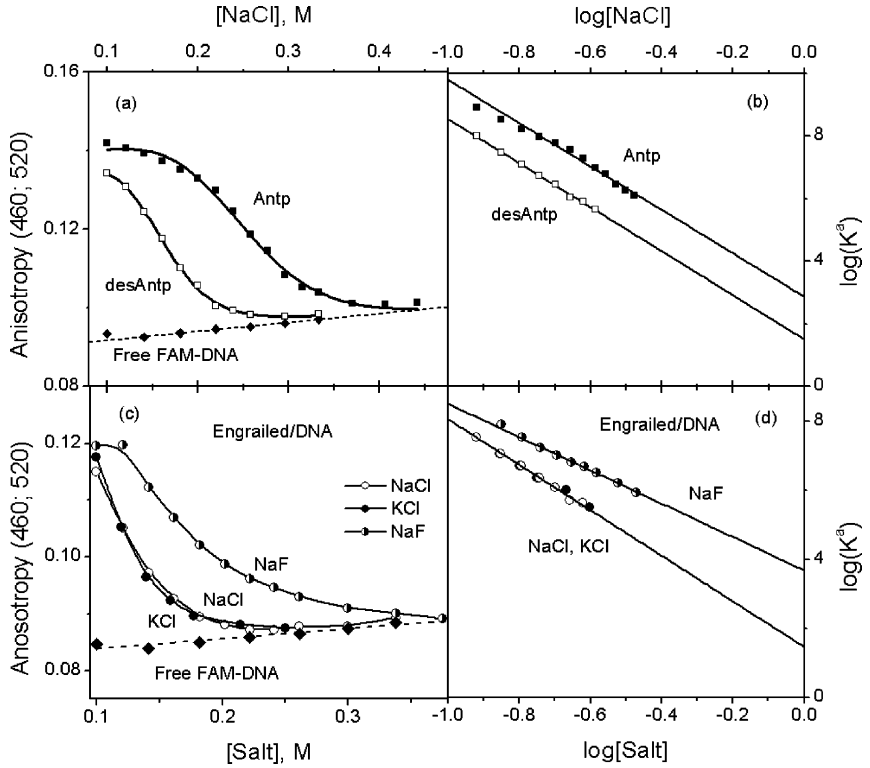

FIGURE 7: (a) Change of anisotropy of the Antp and desAntp complexes at 20 °C in 20 mM sodium acetate at pH 5.0 upon an increase of the NaCl concentration. The initial concentration of the complex was 50 nM. The dotted line represents the anisotropy of the free FAM-labeled DNA. (b) Dependence of $\log(K^a)$ on log [NaCl] for the binding of the full and truncated Antp with their cognate DNA at 20 °C. (c) Change of anisotropy of the engrailed complex at 20 °C in 20 mM sodium acetate at pH 5.0 upon an increase of NaCl, KCl, and NaF concentrations. The dotted line represents the anisotropy of the free FAM-labeled DNA. (d) Dependence of $\log(K^a)$ of the engrailed homeodomain on the logarithm of the NaCl, KCl, and NaF salt concentrations, showing the importance of the anion.

homeodomains, as previously observed for other DNA−protein complexes (*25*, *28*, *29*). It is particularly interesting that removal of the N-terminal arm does not change the slope of the $\log(K^a)$ dependence on log [NaCl] but leads to a parallel shift of this function; i.e., at log [NaCl] = 0 (1 M NaCl), the value of $\log(K^a)_o$ is smaller. A similar situation was found for the truncation of the N-terminal arm of NK-2 (see Table 2).

Figure 7c shows for the example of the engrailed homeodomain that the effect of NaF on the dissociation of the homeodomain complexes is much lower than that of NaCl or KCl. Thus, the dependence of $\log(K^a)$ on the logarithm of the NaF concentration is less steep, and it is the same for KCl as for NaCl (Figure 7d). Thus, the association constants do not depend upon the monovalent cation used but do depend upon the anion.

The logarithm of association constants in 100 mM NaCl, the slopes of their functional dependence on the logarithm of the salt concentration, i.e., $\partial\log(K^a)/\partial\log$ [NaCl], and the extrapolated values of the logarithm of the association constant at log [NaCl] = 0, $\log(K^a)_o$, for all of the considered homeodomains and their truncated forms, are all listed in Table 2.

Gibbs Energies and Entropies of Association. From the measured association constants, the Gibbs energies of associations were calculated as $\Delta G^a(T) = -RT \ln(K^a)$, and when the measured enthalpy is combined with the Gibbs energy of binding, the entropy of binding follows $\Delta S = (\Delta H - \Delta G)/T$. It should be noted that, because Gibbs energies of helix refolding are very small at room temperature (*27*), the Gibbs energy of association does not require correction for the refolding of the recognition helix upon binding to DNA. Furthermore, the small Gibbs energy of helix refolding means that their enthalpic and entropic terms are in balance: thus, if we use enthalpies of association that have been corrected for refolding, $\Delta H^a(T)_{corr}$, the entropies calculated from them will also correspond to the association of the refolded protein with DNA. All of the thermodynamic parameters for association of the refolded homeodomains with their cognate DNAs are listed in Table 3.

Table 3: Thermodynamic Parameters of Association of the Homeodomains with Their Cognate DNAs at 20 °C in 100 mM NaCl and 20 mM Na/Acetate at pH 5.0[a]

	total			electrostatic	nonelectrostatic		
protein	ΔG	ΔH	$-T\Delta S$	$\Delta G_{el} = -T\Delta S_{el}$	ΔG_{nel}	ΔH_{nel}	$-T\Delta S_{nel}$
Antp	−54.3	−12.0	−42.3	−38.6	−15.7	−12.0	−3.7
desAntp	−47.6	−7.0	−40.6	−39.2	−8.4	−7.0	−1.4
NK-2	−51.3	−24.0	−27.3	−30.3	−21.0	−24.0	3.0
desNK-2	−40.6	−16.0	−24.6	−31.3	−9.3	−16.0	6.7
MATα2	−49.8	−26.0	−23.8	−32.5	−17.3	−26.0	8.7
engrailed	−45.1	−19.0	−26.1	−36.9	−8.2	−19.0	10.8
σ	±1.0	±1.0	±2.0	±2.0	±2.0	±1.0	±3.0

[a] ΔG, ΔH, and $T\Delta S$ are in kJ/mol. ΔH values were obtained from ITC measurements. ΔG values were calculated from the K^a values obtained from fluorescence anisotropy titrations. $T\Delta S$ values were obtained by calculation from the equation $T\Delta S = \Delta H - \Delta G$. ΔG_{nel} is calculated from $(K^a)_o$ because this represents the binding constant in 1 M NaCl where electrostatic contributions have become 0. Subtraction of ΔG_{nel} from ΔG gives ΔG_{el}, which equals $-T\Delta S_{el}$ because there is no enthalpic contribution to the electrostatic interactions. Because the measured enthalpy is all nonelectrostatic, combining ΔH_{nel} with ΔG_{nel} yields the nonelectrostatic entropy factor $T\Delta S_{nel}$.

DISCUSSION

Ions Removed on Homeodomain/DNA Association. A linear dependence between the log of the binding constant of a protein with DNA and the log of the salt concentration (e.g., parts b and d of Figure 7) is usually regarded as a manifestation of the electrostatic interactions in this process (*30*−*32*). Formation of ion pairs between the cationic amino acids of the protein (K and R) and the DNA phosphates results in the release of counterions, the mixing of which with the ions in bulk solution produces a significant entropy increase (*30*). At relatively low concentrations of salt in aqueous solution, when the activity of water is minimally affected by the presence of salt, the entropy of water release upon protein binding is independent of the salt concentration, and this entropy effect is simply proportional to the number of released counterions (*33*). Correspondingly, the logarithm of the association constant of protein with DNA is presented in just two terms

$$\log(K^{a}) = \log(K^{a}_{nel}) - (Z\psi + \beta) \log [NaCl] \qquad (1)$$

The first term on the right-hand side results from the nonelectrostatic (nel) interactions between the DNA and protein, and the second results from the electrostatic effects associated with the release of counterions. Here, Z is the number of DNA phosphates that interact with the protein, and ψ is the number of cations per phosphate released upon protein binding, while β is the number of anions released from the protein upon DNA binding. Thus, the slope of this function, i.e., $\partial \log(K^{a})/\partial \log [NaCl] = (Z\psi + \beta)$, actually gives the total number of counterions released upon protein binding to DNA. According to Table 2, the number of counterions released upon formation of the homeodomain/DNA complexes varies between 5.5 and 7.0. Because the full-length homeodomains and their truncated forms have similar slopes (e.g., Figure 7b), it follows that insertion of the N-terminal extension into the minor groove does not result in the release of counterions. It is therefore contact between the globular part of the homeodomains and DNA that leads to the release of counterions.

The contacts formed between the homeodomains and DNA in their complexes can be estimated from the contact maps presented in Figure 2, which show the relative changes of ASA of individual amino acid residues upon association with DNA. From this analysis, it appears that the number of contacts of positively charged residues (i.e., R + K) with DNA phosphates (bars with asterisks in Figure 2) varies between 4 and 6. It has been shown that upon protein association with short DNA duplexes the number of released counterions, ψ, is about 0.64/phosphate (*34*), from which it follows that from 2 to 4 cations should be released from the DNA phosphates upon binding the homeodomains. These values are considerably less than the experimentally determined numbers of ions released upon formation of the homeodomain complexes, 5.5−7.0 (Table 2). This lack of correspondence between the observed number of ions released and the number of ionic phosphate contacts seen in the structures was not the case in our previous studies of forming HMG box/DNA (*29*) or bZIP/DNA (*28*) complexes, for which a good correspondence was observed. The explanation must be that upon formation of the homeodomain/DNA complexes not all of the ions released are cations from the DNA phosphates but some must come from the protein and are anions (*35*, *36*). Indeed, Figure 7d shows that the slope of the $\log(K^{a})$ against log [salt] plot is less when the anion is fluoride than when it is chloride but is independent of the nature of the monovalent cation. For example, in the case of engrailed, the number of released counterions in the NaF solution was found to be 4.5 instead of 6.6 in NaCl and KCl solutions. According to the contact map of the Engrailed complex, Arg and Lys residues form 6 contacts with the DNA phosphates. Because $\psi = 0.64$, this should result in the release of about 4 cations, i.e., close to that found in the NaF solution. Specificity of the homeodomain interaction with the chloride anion is confirmed by the greater influence of NaCl upon the stability of the homeodomains relative to NaF (Figure 3d). Binding of chloride ions seems to be a specific property of homeodomains and could be associated with some special arrangement of charges over the recognition helix, from where they are displaced upon submerging this helix deep into the major groove of DNA. Currently, the ability of DNA-binding proteins to discriminate the nature of bound anions has been reported only for the Ku heterodimer (*37*).

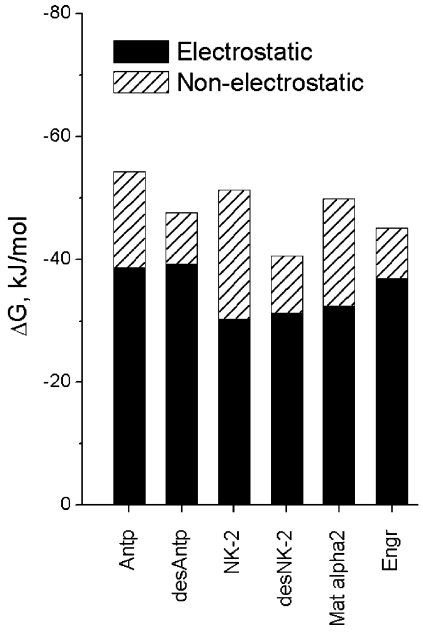

FIGURE 8: Electrostatic and nonelectrostatic components of the Gibbs energy of homeodomain association with their cognate DNAs at 20 °C in 100 mM NaCl and 20 mM Na/acetate buffer at pH 5.0.

Factors Responsible for Binding. When the salt concentration approaches 1 M, i.e., log [KCl] = 0 (see Figure 7), the electrostatic term in eq 1 vanishes and ΔG^{a} approaches the nonelectrostatic part of the Gibbs energy of association, $\Delta G^{a} = \Delta G^{a}_{nel} = -2.3RT \log(K^{a})$ (*32*). This permits splitting the observed Gibbs association energy into two components: the nonelectrostatic and the electrostatic, $\Delta G^{a} = \Delta G^{a}_{nel} + \Delta G^{a}_{el}$, and Figure 8 shows that the electrostatic component of the Gibbs energy substantially dominates the nonelectrostatic. It should be noted that in NaCl solutions a significant part of the electrostatic component of the binding energy is provided by the chloride anions released from protein upon DNA binding.

The electrostatic component of the Gibbs energy is a purely entropic effect caused by mixing the released coun-

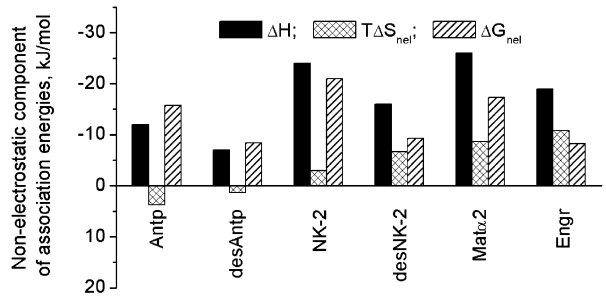

FIGURE 9: Chart showing the nonelectrostatic contributions to the free energies (ΔG^a_{nel}) of forming the homeodomain complexes with their target DNAs, separated into their enthalpic (ΔH) and entropic ($T\Delta S^a_{nel}$) contributions.

terions with ions in the bulk solution; i.e., its enthalpy component is 0, $\Delta G_{el} = -T\Delta S_{el}$ (*29*, *32*). Thus, the association enthalpy, ΔH^a, is solely a component of the nonelectrostatic Gibbs energy: $\Delta G^a_{nel} = \Delta H^a - T\Delta S^a_{nel}$. Correspondingly, we have, for the nonelectrostatic entropy factor of association, $T\Delta S^a_{nel} = \Delta H^a - \Delta G^a_{nel}$. The values of all contributions to the binding of the homeodomains to their cognate DNAs at 20 °C in 100 mM NaCl are given in Table 3 and shown in Figure 9.

From Table 3, it is seen that the association enthalpies of all of the homeodomains are negative and the entropy factors, $-T\Delta S$, are also negative; i.e., the binding entropies are positive. Thus, both factors favor binding; i.e., complex formation is both enthalpy- and entropy-driven, and the entropy factor dominates. From the large positive overall entropy increase upon binding, it is tempting to conclude that hydrophobic interactions play a significant role in binding because these result in dehydration of contacting apolar groups with a consequent increase in the water entropy. This conclusion seems to be confirmed by the negative heat capacity effect of binding the homeodomains, a feature specific for the dehydration of apolar groups (*22*, *38*, *39*). It appears, however, that the positive entropy of binding is provided largely by the release of counterions, while the nonelectrostatic component of the binding entropy, which includes the effect of dehydration of the groups at the interface, is close to 0 and even negative in the case of NK2, MATα2, and Engr (see Table 3). This does not mean that formation of the complexes does not result in dehydration of groups forming the interface but that this positive dehydration entropy effect is more than counterbalanced by the negative entropy cost of association of two kinetic units and the reduction in conformational freedom of groups in the complex.

Because the enthalpy of hydrophobic interactions (i.e., the net enthalpy of formation of van der Waals contact between apolar groups and the dehydration of these groups) is known to be close to 0 at 20 °C (*22*), the observed negative enthalpies of binding at that temperature must result mainly from hydrogen bonding between the protein and DNA. The enthalpy of hydrogen-bond formation at 20 °C is about −3 kJ/mol (*27*); therefore, one can expect formation of 3−9 hydrogen bonds at the association of the homeodomains with DNA. For example, in the case of the Antp/DNA complex, the crystal structure (*48*) shows that three residues make direct hydrogen bonds to the DNA: Arg5 in the minor groove, Ile47 and Asn51 in the major groove, and last being bifurcated. If that is taken to represent 4 hydrogen bonds, the binding enthalpy at 20 °C should be about −12 kJ/mol, which corresponds well with the observed value (see Table 3).

The electrostatic component of the total free energy of homeodomain binding to DNA varies between −30 and −39 kJ/mol, representing 60−80% of the total binding energy, thus dominating the nonelectrostatic component. Nevertheless, the nonelectrostatic component is of special interest because of the widely accepted assumption that it is this component of the binding energy that determines the specificity of DNA recognition (*17*, *29*, *40*−*44*).

Contribution of the N-Terminal Arms to Homeodomain Stability and DNA-Binding Ability. One of the most surprising features of the free NK-2 and Antp homeodomains is that the stability of their truncated forms that lack the N-terminal arm is higher by about 2 kJ/mol than that of the complete homeodomain (Table 1 and parts a and c of Figure 3), with a corresponding increases in T_t of about 3.5 °C. This implies that the charged N-terminal extensions interact with the folded domains into which they induce some stress. This is an unusual situation and not the case for the HMG box proteins Lef-1 or HMG-D for which the removal of the long highly charged C-terminal tails makes no difference to the stability of the folded domains (*26*, *29*) nor is it the case for the globular domains of the linker histones H1 and H5, which also have an unchanged stability following the removal of both of their N- and C-terminal tails (*45*). The N-terminal extension appears unfolded in the free homeodomains, in particular, the segment 1−6 of Antp, as judged from NMR spectra (*46*, *47*). The observation that the destabilizing effect of the arms does not depend upon the salt concentration (see Figure 3c) excludes its simple explanation as a charge-repulsion effect. A detailed understanding of this unusual effect will require a detailed investigation of the solution structure of the full and truncated homeodomains.

It is remarkable that the DNA binding of the highly charged arms of the Antp and NK-2 homeodomains does not result in the release of counterions; i.e., their charges do not contact the DNA phosphates and do not therefore contribute anything to the electrostatic component of the Gibbs energy of binding. Moreover, their binding is mostly enthalpic and proceeds with a negative heat capacity effect (Table 2), implying that it involves the formation of hydrogen bonds and hydrophobic contacts. This is in accordance with the crystallographic information, indicating that the N-terminal arms of homeodomains contact the DNA bases in the minor groove but not the phosphates (*1*, *3*−*6*, *8*, *13*). Correspondingly, the contribution of the N-terminal arm to the stabilization of the homeodomain−DNA complex is sequence-specific, in contrast to HMG boxes where the basic extensions display purely entropic, nonsequence-specific electrostatic interactions with the DNA phosphates (*29*).

CONCLUSIONS

The combination of optical and microcalorimetric experiments enabled us, after the correction for protein refolding, to demonstrate a considerable uniformity in the energetic parameters that drive homeodomain binding to DNA, a situation not apparent from previously published data. In particular, when a comparison is made in the standard buffer

containing 100 mM NaCl, the binding enthalpies cover a quite narrow range, from −12 to −26 kJ/mol at 20 °C, for the complete homeodomains (i.e., with their arms intact) and the ΔC_p values range only from −1.25 to −1.60 kJ/(K mol). The Gibbs energies of binding vary by <10% from the mean, and the dominating electrostatic contribution represents from 60 to 80% of the total. Of particular interest is the observation that this large electrostatic contribution does not derive solely from the release of cations from the DNA phosphates, in the manner previously found for HMG boxes, but contains a significant contribution from the release of the anions (chloride) from the protein on forming the complex. The other important finding is that the effects of the N-terminal arms on DNA binding are entirely nonelectrostatic: despite their high positive charge, they do not displace cations from the DNA but make sequence-specific hydrophobic contacts and form hydrogen bonds in the minor groove; i.e., the contribution of the N-terminal arms of homeodomains to the stabilization of their DNA complexes differs qualitatively from that of the long basic extensions of HMG boxes that interact nonsequence-specifically with DNA phosphates by entirely entropic forces. It appears therefore that, while DBDs frequently have basic extensions to their folded domains, these can use two very different strategies to increase the binding affinity, and in the case of the homeodomains, the extensions also make a contribution to specificity, unlike those of the HMG box-containing proteins.

ACKNOWLEDGMENT

We thank Dr. Alexander Johnson, Dr. Walter Gehring, Dr. Neil Clarke, and Dr. James Ferretti for providing us with the expression plasmids used in this work. The financial support of the NIH (GM48036) is gratefully acknowledged.

REFERENCES

1. Fraenkel, E., Rould, M. A., Chambers, K. A., and Pabo, C. O. (1998) Engrailed homeodomain−DNA complex at 2.2 Å resolution: A detailed view of the interface and comparison with other engrailed structures, *J. Mol. Biol. 284*, 351−361.
2. Gruschus, J. M., Tsao, D. H., Wang, L. H., Nirenberg, M., and Ferretti, J. A. (1997) Interactions of the vnd/NK-2 homeodomain with DNA by nuclear magnetic resonance spectroscopy: Basis of binding specificity, *Biochemistry 36*, 5372−5380.
3. Kissinger, C. R., Liu, B. S., Martin-Blanco, E., Kornberg, T. B., and Pabo, C. O. (1990) Crystal structure of an engrailed homeodomain−DNA complex at 2.8 Å resolution: A framework for understanding homeodomain−DNA interactions, *Cell 63*, 579−590.
4. Otting, G., Qian, Y. Q., Billeter, M., Muller, M., Affolter, M., Gehring, W. J., and Wuthrich, K. (1990) Protein−DNA contacts in the structure of a homeodomain−DNA complex determined by nuclear magnetic resonance spectroscopy in solution, *EMBO J. 9*, 3085−3092.
5. Qian, Y. Q., Furukubo-Tokunaga, K., Resendez-Perez, D., Muller, M., Gehring, W. J., and Wuthrich, K. (1994) Nuclear magnetic resonance solution structure of the fushi tarazu homeodomain from *Drosophila* and comparison with the Antennapedia homeodomain, *J. Mol. Biol. 238*, 333−345.
6. Qian, Y. Q., Resendez-Perez, D., Gehring, W. J., and Wuthrich, K. (1994) The des(1−6)antennapedia homeodomain: Comparison of the NMR solution structure and the DNA-binding affinity with the intact Antennapedia homeodomain, *Proc. Natl. Acad. Sci. U.S.A. 91*, 4091−4095.
7. Tsao, D. H., Gruschus, J. M., Wang, L. H., Nirenberg, M., and Ferretti, J. A. (1994) Elongation of helix III of the NK-2 homeodomain upon binding to DNA: A secondary structure study by NMR, *Biochemistry 33*, 15053−15060.
8. Wolberger, C., Vershon, A. K., Liu, B., Johnson, A. D., and Pabo, C. O. (1991) Crystal structure of a MATα2 homeodomain−operator complex suggests a general model for homeodomain−DNA interactions, *Cell 67*, 517−528.
9. Carra, J. H., and Privalov, P. L. (1997) Energetics of folding and DNA binding of the MATα2 homeodomain, *Biochemistry 36*, 526−535.
10. Tsao, D. H., Gruschus, J. M., Wang, L. H., Nirenberg, M., and Ferretti, J. A. (1995) The three-dimensional solution structure of the NK-2 homeodomain from *Drosophila*, *J. Mol. Biol. 251*, 297−307.
11. Wolberger, C. (1996) Homeodomain interactions, *Curr. Opin. Struct. Biol. 6*, 62−68.
12. Gonzalez, M., Weiler, S., Ferretti, J. A., and Ginsburg, A. (2001) The vnd/NK-2 homeodomain: thermodynamics of reversible unfolding and DNA binding for wild-type and with residue replacements H52R and H52R/T56W in helix III, *Biochemistry 40*, 4923−4931.
13. Ke, A., Mathias, J. R., Vershon, A. K., and Wolberger, C. (2002) Structural and thermodynamic characterization of the DNA binding properties of a triple alanine mutant of MATα2, *Structure 10*, 961−971.
14. Ladbury, J. E., Wright, J. G., Sturtevant, J. M., and Sigler, P. B. (1994) A thermodynamic study of the trp repressor−operator interaction, *J. Mol. Biol. 238*, 669−681.
15. Merabet, E., and Ackers, G. K. (1995) Calorimetric analysis of λ cI repressor binding to DNA operator sites, *Biochemistry 34*, 8554−8563.
16. Privalov, P. L., Jelesarov, I., Read, C. M., Dragan, A. I., and Crane-Robinson, C. (1999) The energetics of HMG box interactions with DNA: Thermodynamics of the DNA binding of the HMG box from mouse sox-5, *J. Mol. Biol. 294*, 997−1013.
17. Takeda, Y., Ross, P. D., and Mudd, C. P. (1992) Thermodynamics of Cro protein−DNA interactions, *Proc. Natl. Acad. Sci. U.S.A. 89*, 8180−8184.
18. Weiler, S., Gruschus, J. M., Tsao, D. H., Yu, L., Wang, L. H., Nirenberg, M., and Ferretti, J. A. (1998) Site-directed mutations in the vnd/NK-2 homeodomain. Basis of variations in structure and sequence-specific DNA binding, *J. Biol. Chem. 273*, 10994−11000.
19. Privalov, G., Kavina, V., Freire, E., and Privalov, P. L. (1995) Precise scanning calorimeter for studying thermal properties of biological macromolecules in dilute solution, *Anal. Biochem. 232*, 79−85.
20. Privalov, P. L., and Potekhin, S. A. (1986) Scanning microcalorimetry in studying temperature-induced changes in proteins, *Methods Enzymol. 131*, 4−51.
21. Makhatadze, G. I., Kim, K. S., Woodward, C., and Privalov, P. L. (1993) Thermodynamics of BPTI folding, *Protein Sci. 2*, 2028−2036.
22. Makhatadze, G. I., and Privalov, P. L. (1995) Energetics of protein structure, *Adv. Protein Chem. 47*, 307−425.
23. Hackel, M., Hinz, H. J., and Hedwig, G. R. (1999) A new set of peptide-based group heat capacities for use in protein stability calculations, *J. Mol. Biol. 291*, 197−213.
24. Privalov, P. L., and Makhatadze, G. I. (1990) Heat capacity of proteins. II. Partial molar heat capacity of the unfolded polypeptide chain of proteins: Protein unfolding effects, *J. Mol. Biol. 213*, 385−391.
25. Dragan, A. I., Liggins, J. R., Crane-Robinson, C., and Privalov, P. L. (2003) The energetics of specific binding of AT-hooks from HMGA1 to target DNA, *J. Mol. Biol. 327*, 393−411.
26. Dragan, A. I., Klass, J., Read, C., Churchill, M. E., Crane-Robinson, C., and Privalov, P. L. (2003) DNA binding of a non-sequence-specific HMG-D protein is entropy driven with a substantial non-electrostatic contribution, *J. Mol. Biol. 331*, 795−813.
27. Taylor, J. W., Greenfield, N. J., Wu, B., and Privalov, P. L. (1999) A calorimetric study of the folding-unfolding of an α-helix with covalently closed N- and C-terminal loops, *J. Mol. Biol. 291*, 965−976.
28. Dragan, A. I., Frank, L., Liu, Y., Makeyeva, E. N., Crane-Robinson, C., and Privalov, P. L. (2004) Thermodynamic signature of GCN4-bZIP binding to DNA indicates the role of water in discriminating between the AP-1 and ATF/CREB sites, *J. Mol. Biol. 343*, 865−878.
29. Dragan, A. I., Read, C. M., Makeyeva, E. N., Milgotina, E. I., Churchill, M. E., Crane-Robinson, C., and Privalov, P. L. (2004)

DNA binding and bending by HMG boxes: Energetic determinants of specificity, *J. Mol. Biol. 343*, 371−393.
30. Manning, G. S. (1978) The molecular theory of polyelectrolyte solutions with applications to the electrostatic properties of polynucleotides, *Q. Rev. Biophys. 11*, 179−246.
31. Record, M. T., Jr., Anderson, C. F., and Lohman, T. M. (1978) Thermodynamic analysis of ion effects on the binding and conformational equilibria of proteins and nucleic acids: The roles of ion association or release, screening, and ion effects on water activity, *Q. Rev. Biophys. 11*, 103−178.
32. Record, M. T., Jr., Zhang, W., and Anderson, C. F. (1998) Analysis of effects of salts and uncharged solutes on protein and nucleic acid equilibria and processes: A practical guide to recognizing and interpreting polyelectrolyte effects, Hofmeister effects, and osmotic effects of salts, *Adv. Protein Chem. 51*, 281−353.
33. Ha, J. H., Capp, M. W., Hohenwalter, M. D., Baskerville, M., and Record, M. T., Jr. (1992) Thermodynamic stoichiometries of participation of water, cations and anions in specific and nonspecific binding of lac repressor to DNA. Possible thermodynamic origins of the "glutamate effect" on protein−DNA interactions, *J. Mol. Biol. 228*, 252−264.
34. Olmsted, M. C., Bond, J. P., Anderson, C. F., and Record, M. T., Jr. (1995) Grand canonical Monte Carlo molecular and thermodynamic predictions of ion effects on binding of an oligocation ($L8^+$) to the center of DNA oligomers, *Biophys. J. 68*, 634−647.
35. Overman, L. B., and Lohman, T. M. (1994) Linkage of pH, anion, and cation effects in protein−nucleic acid equilibria. *Escherichia coli* SSB protein−single stranded nucleic acid interactions, *J. Mol. Biol. 236*, 165−178.
36. Record, M. T., Jr., Ha, J. H., and Fisher, M. A. (1991) Analysis of equilibrium and kinetic measurements to determine thermodynamic origins of stability and specificity and mechanism of formation of site-specific complexes between proteins and helical DNA, *Methods Enzymol. 208*, 291−343.
37. Arosio, D., Costantini, S., Kong, Y., and Vindigni, A. (2004) Fluorescence anisotropy studies on the Ku−DNA interaction: Anion and cation effects, *J. Biol. Chem. 279*, 42826−42835.
38. Privalov, P. L., and Makhatadze, G. I. (1992) Contribution of hydration and non-covalent interactions to the heat capacity effect on protein unfolding, *J. Mol. Biol. 224*, 715−723.
39. Spolar, R. S., Livingstone, J. R., and Record, M. T., Jr. (1992) Use of liquid hydrocarbon and amide transfer data to estimate contributions to thermodynamic functions of protein folding from the removal of nonpolar and polar surface from water, *Biochemistry 31*, 3947−3955.
40. Boschelli, F. (1982) λ-Phage Cro-repressor−Non-specific DNA-binding, *J. Mol. Biol. 162*, 267−282.
41. Dehaseth, P. L., Lohman, T. M., and Record, M. T. (1977) Nonspecific interaction of lac repressor with DNA−Association reaction driven by counterion release, *Biochemistry 16*, 4783−4790.
42. Ha, J. H., Spolar, R. S., and Record, M. T., Jr. (1989) Role of the hydrophobic effect in stability of site-specific protein−DNA complexes, *J. Mol. Biol. 209*, 801−816.
43. Matthew, J. B., and Ohlendorf, D. H. (1985) Electrostatic deformation of DNA by a DNA-binding protein, *J. Biol. Chem. 260*, 5860−5862.
44. Revzin, A., and von Hippel, P. H. (1977) Direct measurement of association constants for the binding of *Escherichia coli* lac repressor to non-operator DNA, *Biochemistry 16*, 4769−4776.
45. Tiktopulo, E. I., Privalov, P. L., Odintsova, T. I., Ermokhina, T. M., Krasheninnikov, I. A., Aviles, F. X., Cary, P. D., and Crane-Robinson, C. (1982) The central tryptic fragment of histones H1 and H5 is a fully compacted domain and is the only folded region in the polypeptide chain. A thermodynamic study, *Eur. J. Biochem. 122*, 327−331.
46. Qian, Y. Q., Billeter, M., Otting, G., Muller, M., Gehring, W. J., and Wuthrich, K. (1989) The structure of the Antennapedia homeodomain determined by NMR spectroscopy in solution: Comparison with prokaryotic repressors, *Cell 59*, 573−580.
47. Qian, Y. Q., Otting, G., Furukubo-Tokunaga, K., Affolter, M., Gehring, W. J., and Wuthrich, K. (1992) NMR structure determination reveals that the homeodomain is connected through a flexible linker to the main body in the *Drosophila* Antennapedia protein, *Proc. Natl. Acad. Sci. U.S.A. 89*, 10738−10742.
48. Fraenkel, E., and Pabo, C. O. (1998) Comparison of X-ray and NMR structures for the Antennapedia homeodomain−DNA complex, *Nat. Struct. Biol. 5*, 692−697.

BI051705M